

Higher d.c. resistivity of Li–Zn–Cd ferrites prepared by microwave sintering compared with conventional sintering

MAMATA MAISNAM* and SUMITRA PHANJOBAM

Department of Physics, Manipur University, Canchipur, Imphal 795 003, India

MS received 8 April 2013; revised 27 September 2013

Abstract. Cd^{2+} -substituted Li–Zn ferrites having the general formula $\text{Li}_{0.4-x/2}^+\text{Zn}_{0.2}^{2+}\text{Cd}_x^{2+}\text{Fe}_{2.4-x/2}^{3+}\text{O}_4^{2-}$ where $x = 0.02, 0.03$ and 0.04 have been prepared by both microwave sintering and conventional sintering. In the former case, sintering was done at 1050°C for 25 min, whereas in the latter case sintering was done at 1050°C for 6 h. The various structural properties, microstructures and d.c. resistivity of the samples prepared by the two techniques were compared. The study showed higher d.c. resistivity and higher activation energies in the samples prepared by microwave sintering. The mechanisms pertaining to the results are discussed.

Keywords. Ceramics; lithium ferrites; spinel structure; microwave sintering; d.c. resistivity; activation energy.

1. Introduction

Lithium ferrites are good dielectric materials with interesting magnetic properties like high Curie temperature, rectangularity of hysteresis loop and high saturation magnetization, thereby making them technically very promising low-cost material for microwave devices (Baba *et al* 1972; Argentina and Baba 1974). However, one major limitation from broad utilization of these materials is their low electrical resistivity, high dielectric and magnetic losses. This is because of excessive loss of lithium and oxygen during sintering, resulting in non-stoichiometric, low density, high porosity and high loss characteristics (Ridgley *et al* 1970; Bandyopadhyay and Fulrath 1974; Kishan *et al* 1981). To be useful in many applications, it is highly demanding that the d.c. resistivity be raised in addition to the improvements in the afore-mentioned properties. This attempt may be achieved by adopting different methodological approaches such as different preparation methods, different sintering techniques, controlling sintering temperatures and atmospheres and additions of minor substituent (Wang *et al* 1968; Kishan 1993).

Microwave-sintering technique using microwave energy for sintering advanced ceramics has been well reported recently (Yadogi *et al* 2003; Tsakaloudi *et al* 2004). It is a very convenient method and has several potential advantages over the conventional sintering technique. The microwave kilns are of significantly reduced size and

easy to handle than the conventional one. The advantages of this technique include even and rapid heating, eco-friendliness, improved processing efficiencies and energy saving. This method is advantageous in terms of sintering cycle time, energy efficiency and cost. The resulting product has finer and more uniform microstructures leading to improved properties like density, stoichiometry, electrical, magnetic and mechanical properties. Microwave-sintering technique efficiently prevents material loss during processing and, therefore, it is advantageous in upgrading various properties, especially the stoichiometry and electrical resistivity. Improvement in various properties being obtained in Li–Ni–Mn ferrite system prepared by microwave-sintering technique over conventional sintering was reported elsewhere (Maisnam *et al* 2005). Zn^{2+} -substituted Li-ferrites have been extensively studied because of their potential applications in microwave devices (Baba *et al* 1972; Rezlescu *et al* 1974; White and Patton 1978; Raman and Murthy 1990). Cd^{2+} ions like Zn^{2+} ions keep their divalency, have strong preferences for the tetrahedral sites of the crystal lattice and produce beneficial effects on the atomic diffusibility, sintering kinetics and microstructures. Cd^{2+} substitution in Li-ferrites were studied with much interest by many workers as it helps in enhancing resistivity, initial permeability, saturation magnetization, etc. – the important properties that determine their applicability in microwave devices (Ravinder 1994, Bellad *et al* 1999, 2000; Akhtar *et al* 2009). Sagare *et al* (1997) studied the electrical switching and memory phenomena in Li–Cd ferrites. Structural and electrical properties of small amount of Cd^{2+} -substituted Li–Zn ferrites prepared by conventional

*Author for correspondence (m_maisnam@yahoo.co.in)

technique was reported elsewhere (Maisnam *et al* 2010). However, no reports have been found on the study of the effect of microwave sintering on the various parameters of these systems. In the present paper, it is aimed to study the higher d.c. resistivity achieved in Cd^{2+} -substituted Li–Zn ferrites when prepared by microwave sintering.

2. Experimental

Polycrystalline Cd^{2+} -substituted Li–Zn ferrites having the compositional formula $\text{Li}_{0.4-x/2}\text{Zn}_{0.2}\text{Cd}_x\text{Fe}_{2.4-x/2}\text{O}_4$ where $x = 0.02, 0.03$ and 0.04 have been prepared by the ceramic method. High-purity AR grade chemicals, viz. Li_2CO_3 , ZnO , CdO , Fe_2O_3 , were taken in stoichiometric ratio, ball-milled with distilled water for 10 h. The mixture was dried, ground to smooth powder and calcined at 850°C for 6 h. A small amount of Bi_2O_3 (0.5 wt%) was added to the calcined powder as a sintering aid. The mixture was ball-milled again for 10 h, dried and ground to smooth powder. The powder was mixed with 3 wt% PVA as a binder and pressed into compact pellets with an applied pressure of 50 kN for 3 min. One set of the compositions was sintered using a microwave furnace at 1050°C (heating rate of $50^\circ\text{C}/\text{min}$) for 25 min and then furnace cooled. The samples were named as S1(m), S2(m) and S3(m) for $x = 0.02, 0.03$ and 0.04 , respectively. Another set was sintered using the conventional furnace at 1050°C for 6 h (heating rate of $5^\circ\text{C}/\text{min}$) and, then, furnace cooled and correspondingly named as S1(c), S2(c) and S3(c) for the different amounts of Cd^{2+} concentration. The sintered pellets were then polished to be used for further measurements. XRD was taken to confirm the phase structure using Philips Analytical X'PERT PRO. The lattice constant, a , and theoretical densities, d_x , were determined from the XRD data. Bulk density, d , was measured using Archimedes principle. Porosity of the samples was measured using the formula, $P = (d_x - d)/d_x$. Scanning electron microscope (SEM Quanta 250) took the photomicrographs on the fractured surface of the samples. Curie temperature was measured using Soohoo's method (Soohoo 1960). This method is also known as 'sample drop method'. In this method, a small piece of sample was attached to a very strong magnet. Using a heating chamber, the temperature of the sample was raised and a standard thermocouple measured the temperature of the sample. When the temperature of the sample was raised high enough, at a particular temperature the sample falls off from the magnet and the temperature is recorded. This temperature indicates the Curie temperature of the sample. Electrical contacts were made on both sides of the flat surfaces of the pellets to use in electrical measurements. Room temperature d.c. resistivity was determined using the standard two-probe method and a Keithley electrometer. D.C. resistivity was also measured as a function of temperature from room temperature to

423 K . For this, the cell along with the sample was placed inside a beaker containing oil medium and the beaker was heated using a simple heating chamber. Sample was heated in oil medium to ensure uniform heating. A standard thermocouple was used to measure the temperature of the sample with the thermocouple wire dipped into the beaker containing cell and kept at a distance of about 0.1 cm away from the sample to avoid any voltage pick-up. As we increased the temperature, measurement was taken in such a way that sufficient time was allowed to obtain thermal equilibrium in the cell and more sufficiently in the sample before the resistance value was recorded. From the value of resistance, the d.c. resistivity (ρ) was calculated using the dimension of the sample in the formula, $\rho = RA/t$, where R is the resistance value, A the area and t the thickness of the sample. A linear curve of $\log \rho$ vs $1000/T$ was plotted, from which activation energy, E_ρ , was determined using the Arrhenius formula, $\rho = \rho_0 \exp\{-E_\rho/kT\}$, where T is the absolute temperature, ρ_0 a temperature-independent constant which is a function of the nature of the material and k the Boltzmann constant.

3. Results and discussion

XRD images have confirmed the formation of a single-phase with spinel structure for all the samples and XRD patterns for the samples are shown in figure 1. The observation of the patterns showed higher-intensity peaks for the microwave-sintered samples (m-samples) compared with the conventional-sintered samples (c-samples) indicating better crystallization in the former process (Wang *et al* 1968; Samasekara and Cadieu 2001). A comparative study of the structural information, viz. lattice constant, a , theoretical density were done and tabulated in table 1. For both the sintering techniques, a increased with increase of Cd^{2+} substitution, which may be due to increasing substitution of larger ions. This can be understood by the

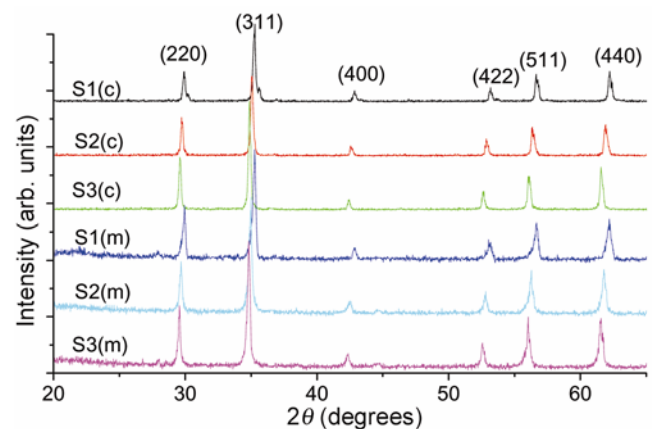


Figure 1. XRD pattern for the microwave-sintered (S1(m), S2(m), S3(m)) and conventional-sintered (S1(c), S2(c), S3(c)) $\text{Li}_{0.4-x/2}\text{Zn}_{0.2}\text{Cd}_x\text{Fe}_{2.4-x/2}\text{O}_4$ ferrites.

Table 1. Structural properties of microwave- and conventional-sintered $\text{Li}_{0.4-x/2}\text{Zn}_{0.2}\text{Cd}_x\text{Fe}_{2.4-x/2}\text{O}_4$ ferrites.

Sample	Lattice constant, a (Å)		X-ray density, d_x (g/cc)		Experimental density, d (g/cc)		Porosity (%)	
	c	m	c	m	c	m	c	m
S1	8.437	8.438	5.235	5.233	4.941	4.958	5.62	5.25
S2	8.485	8.512	5.296	5.248	4.989	4.969	5.79	5.31
S3	8.519	8.544	5.389	5.337	5.057	5.041	6.16	5.55

progressive substitution of the larger ionic size atoms replacing the smaller ones. From the compositional formula of the present system, $\text{Li}_{0.4-x/2}\text{Zn}_{0.2}\text{Cd}_x\text{Fe}_{2.4-x/2}\text{O}_4^{2-}$, it can be seen that two Cd^{2+} ions with the ionic radius 1.09 Å, i.e. 2.18 Å are substituting a combination ($\text{Li}^+ + \text{Fe}^{3+}$) ions of average ionic radius 1.41 Å (ionic radii of Li^+ and Fe^{3+} are 0.74 and 0.67 Å, respectively) (Gorter 1954). The increase in a is therefore expected as observed. Also, increase in density with increase in Cd^{2+} substitution may be due to progressive substitution of heavier ions (Cd^{2+} ions) substituting the lighter ones (Li^+ and Fe^{3+}) (Maisnam *et al* 2010). Table 1 further shows that the theoretical densities as well as the experimental densities of the c-samples and m-samples are closely comparable. However, porosity is slightly reduced with microwave sintering (table 1). Processing duration is very short in microwave sintering, and therefore has very little chance of material volatilization. In conventional sintering, prolonged sintering may lead to evaporation of constituent material, leaving behind intragranular pores that get trapped in the bulk resulting in raising the porosity.

Typical SEM photomicrographs for all the samples are shown in figure 2. The microstructural study of the samples from photomicrographs revealed that the microwave-sintered samples showed smaller grains compared to conventionally sintered counterparts. Microwave sintering which completed within a few minutes of processing offer limited duration for grain growth and therefore produced refinement of microstructures with smaller grains compared with long hours of conventional sintering availing with sufficient time for large-size grain growth (figure 2). It is also seen that the sizes of pores between the grains are also smaller in the microwave-sintered samples indicating a greater degree of compactness of the grains.

Compositional variation of the Curie temperature, T_c depicted in table 2, showed that for both the preparation techniques, Curie temperature decreased with increased Cd^{2+} substitution. This may be due to reduction of Fe^{3+} ions and, hence, reduction of active $\text{Fe}^{3+}-\text{O}^{2-}-\text{Fe}^{3+}$ linkages with increased Cd^{2+} ions substitution as reported elsewhere (Maisnam *et al* 2010). On comparison of the two techniques, it is observed that samples prepared by microwave sintering have slightly higher values of Curie temperature. Curie temperature in Li-ferrites having been decreased with loss of lithium ions during sintering was

reported by others (Rezlescu *et al* 1974). The result showing a small rise in the T_c values may have been due to control of lithium loss by microwave sintering. With lesser lithium loss by microwave sintering, the number of Fe^{3+} ions being converted to Fe^{2+} ions is reduced. Comparatively, the active linkages of Fe^{3+} vis-a-vis O^{2+} ions that determines T_c is higher for m-samples. Hence, the results as obtained.

Room temperature d.c. resistivities are compared and tabulated in table 2. The table showed that the d.c. resistivity of the m-samples is enhanced by one order. Higher resistivity obtained due to microwave sintering was also reported by other workers (Bhasker *et al* 2004). The main mode of conduction in ferrites is the electron exchange between Fe^{2+} and Fe^{3+} ions at the B sites. Li-ferrites tend to lose lithium and oxygen during sintering at high temperature, leading to evolution of Fe^{2+} ions, the charge species responsible for conduction process in Li-ferrites. The oxygen lost however is regained during slow cooling, as reported by Rezlescu *et al* (1974) and Fe^{2+} ions may be oxidized back to Fe^{3+} ions. But the number of Li loss equals the number of Fe^{3+} ions which become Fe^{2+} ions and they reside at B sites promoting electron exchanges. Microwave sintering due to the short processing period might have got very little chance for material losses, leading to the reduction in the number of Fe^{2+} ions formed during sintering. Furthermore, better crystallinity and stoichiometry with finer microstructures of m-samples may also add to the rise in d.c. resistivity. Small grains are more or less spherical in shape and the grain size distribution is more homogeneous. D.C. resistivity of ferrites depends on various microstructural properties like grain size, grain boundaries, porosity and stoichiometry. Smaller grains show greater surface to volume ratio, therefore, oxidation occurs faster and reconversion of Fe^{2+} ions formed during sintering back to Fe^{3+} ions may take place. Hence, the existence of Fe^{2+} ions is lower in smaller microstructured samples (Singh *et al* 2002a). In addition, small grains in particular imply greater number of insulating grain boundaries, which acts as scattering centres to the flow of charge carriers, thereby reducing electron exchanges and, thus, the resistivity is bound to rise (Singh *et al* 2002b; Bhasker *et al* 2004). The results obtained may be due to the contribution of all the above factors. Increase in d.c. resistivity with increase of Cd^{2+}

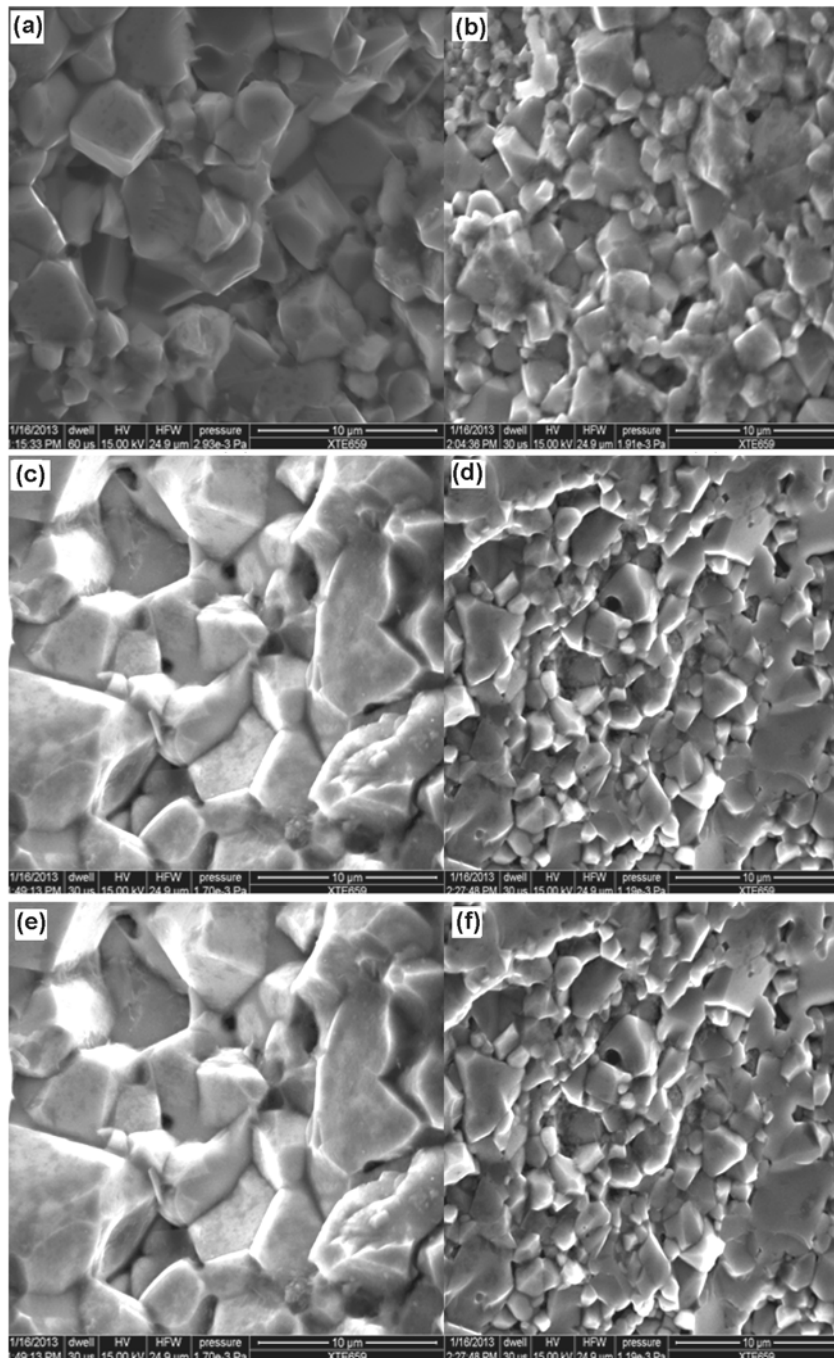
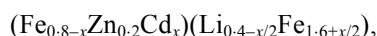


Figure 2. SEM photomicrographs for the conventional-sintered samples: (a) S1(c); (c) S2(c); (e) S3(c) and the microwave-sintered samples: (b) S1(m); (d) S2(m); (f) S3(m).

Table 2. Magnetic and electrical properties of microwave- and conventional-sintered $\text{Li}_{0.4-x/2}\text{Zn}_{0.2}\text{Cd}_x\text{Fe}_{2.4-x/2}\text{O}_4$ ferrites.

Sample	Curie temperature (°C)		D.C. resistivity (Ω-cm)		Activation energy (eV)			
	c	m	c ($\times 10^3$)	m ($\times 10^4$)	c		m	
					Region I	Region II	Region I	Region II
S1	469	471	4.326	9.563	0.072	0.230	0.154	0.386
S2	420	425	6.437	11.612	0.083	0.252	0.158	0.427
S3	355	361	7.969	20.457	0.138	0.294	0.209	0.533

content in Li–Zn ferrites prepared by conventional sintering was reported elsewhere (Maisnam *et al* 2010). Similar results have been obtained when the samples are sintered with microwave technique (table 2). As explained earlier, where Zn^{2+} and Cd^{2+} ions having their strong preferences for the A sites, the expected cation distribution may be written as



where x is the amount of Cd^{2+} ions substituted. With progressive substitution of Cd^{2+} ions, Li^+ ions decrease, while Fe^{3+} ions increase at the B-sites. Decrease in Li ion concentration at the B sites imply reduced chance of Fe^{2+} ions created due to Li evaporation (table 2). Hence, electron exchanges between the iron ions are reduced. The increase in the d.c. resistivity was also reported as contribution from the deviation of structural stoichiometry arising out of the very large ions (Cd^{2+}) trying to occupy the very small tetrahedral sites (Maisnam *et al* 2010).

D.C. resistivity was then studied as a function of temperature from RT to 423 K and the plot of $\log \rho$ vs $1000/T$ for all the compositions is shown in figure 3. Figures showed $\log \rho$ remaining nearly constant with the rise of temperature in the beginning and, then, later on started to decrease with the increase of temperature. Increase of temperature generally increases the mobility of conduction charge species and, therefore, the resistivity decreases. The curve was found to be a straight line and the slope of the curve gives the activation energy using the Arrhenius formula. The slopes of the curves for samples S1(c) and

S1(m), out of which the activation energies were determined, are showed in inset figure (a) of figure 3. Inset figure further showed a change in the slope of the curve at higher temperature region. The temperature at which the slope of the curve changes is higher for the m-samples compared to that for the c-samples. The appearance of two slopes indicated that the resistivity is affected by superposition of a number of thermally activated contributions. The temperature at which the slope changes does not seem to correspond to the Curie temperature as seen in table 2. This indicated that there exist two parallel conduction mechanisms. Conduction in ferrites is due to electron hopping between Fe^{2+} and Fe^{3+} ions at the B sites, but lithium ferrites contain reducible lithium ions besides the iron ions and they thereby exhibit ionic conduction too. The curves may then be divided into two regions: region I or the low-temperature region and region II or high-temperature region. The electron conduction mechanism occurs in region I, while the ionic conduction occurs in region II.

The activation energies for all the other samples were determined in the same manner. The values of activation energy, E_g , for both the regions are tabulated (table 2) and it is observed that they increased with increased substitution. This is because E_g is affected by hopping probability associated with the electrical energy barrier experienced by electrons during hopping. With increased substitution, due to less Fe^{2+} ions available as discussed earlier, the number of hopping pair Fe^{2+} – Fe^{3+} decreased. Consequently, hopping probability decreased and thereby E_g is raised. Increase of lattice constant (table 1) manifest itself the increase of interatomic distances, thereby the barrier in hopping encountered by conduction charges also increases. As such, E_g is increased with increased substitution. The table further shows that microwave-sintered samples had slightly higher value of activation energies than their conventionally sintered counterparts. Besides, interatomic distances activation energy is also affected by the grain structure. Grain size of m-sample is smaller, and smaller grains imply greater number of insulating grain boundaries. Therefore, the contact area for electron hopping between the conducting grain to grain decreases. The hopping of charge species decreased and, hence, the activation is expected to rise as obtained (Singh *et al* 2002b).

4. Conclusions

Structural properties, microstructures and d.c. resistivity of Li–Zn–Cd ferrite having the general formula $\text{Li}_{0.4-x/2}\text{Zn}_{0.2}\text{Cd}_x\text{Fe}_{2.4-x/2}\text{O}_4$ where $x = 0.02, 0.03$ and 0.04 prepared by the microwave-sintering technique have been compared with those obtained from samples of same composition prepared by the conventional-sintering technique. In the former technique, sintering was done at

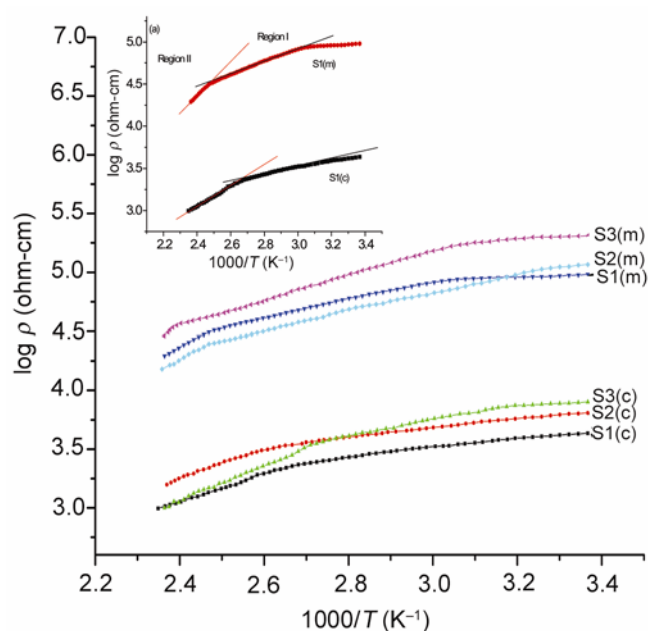


Figure 3. Temperature variation of d.c. resistivity for the microwave- and conventional-sintered $\text{Li}_{0.4-x/2}\text{Zn}_{0.2}\text{Cd}_x\text{Fe}_{2.4-x/2}\text{O}_4$ ferrites. Inset figure (a) shows the slopes of the curves in region I and region II for samples S1(c) and S1(m), respectively.

1050 °C for 25 min, while in the latter case, sintering was done at 1050 °C for 6 h. The d.c. resistivity for the microwave-sintered samples has been enhanced by one order compared with their conventionally sintered counterparts. Activation energies showed higher values for the microwave-sintered samples. Control of material loss, lower porosity and better microstructures with finer grains have contributed to the enhancement in the d.c. resistivity.

Acknowledgement

The authors are thankful to UGC, Delhi, for the financial assistance for the research. The authors also thank Electroceramics Laboratory G V M Girls College, Sonapat, Haryana, for allowing us to carry out microwave-sintering of our samples.

References

- Akhter S, Paul D P, Manjura Hoque S and Hakim M K 2009 *J. Bangla. Acad. Sci.* **33** 159
- Argentina G M and Baba P D 1974 *IEEE Trans. on Microwave Theory and Applications* MTT-22 652
- Baba P D, Argentina G M, Courtney W E, Dionne G F and Temme D H 1972 *IEEE Trans. on Mags.* **MAG-8** 83
- Bandyopadhyay G and Fulrath R M 1974 *J. Am. Ceram. Soc.* **57** 182
- Bellad S S, Watawe S C and Chougula B K 1999 *J. Magn. Mater.* **195** 57
- Bellad S S, Watawe S C, Shaikh A M and Chougula B K 2000 *Bull. Mater. Sci.* **23** 83
- Bhaskar A, Kranth B R and Murthy S R 2004 *J. Mater. Sci.* **39** 3787
- Gorter E W 1954 *Philips Res. Rep.* **9** 318
- Kishan P 1993 *Microwave materials* (New Delhi, India: Narosa Publishing House) p. 141
- Kishan P, Chatterjee S N, Nagpaul L K and Laroia K K 1981 *Ind. J. Pure Appl. Phys.* **19** 83
- Maisnam M, Phanjoubam S and Prakash C 2005 *Mod. Phys. Lett.* **B19** 1051
- Maisnam M, Phanjoubam S and Prakash C 2010 *Mod. Phys. Lett.* **B24** 2195
- Raman R and Murthy V R K 1990 *J. Appl. Phys.* **69** 4053
- Ravinder D 1994 *J. Appl. Phys.* **75** 6121
- Rezlescu N, Condurache D, Petrasiu P and Licia E 1974 *J. Am. Ceram. Soc.* **57** 40
- Ridgley D H, Lessoff H and Childress J D 1970 *J. Am. Ceram. Soc.* **6** 304
- Sagare M S, Vaingankar M S and Kulkarni S G 1997 *J. Phys. IV France* **7** 111
- Samasekara P and Cadieu F J 2001 *Chin. J. Phys.* **39** 635
- Singh A K, Verma A, Thakur O P, Prakash C, Goel T C and Mendiratta R G 2002a *J. Appl. Phys.* **41** 5142
- Singh A K, Goel T C, Mendiratta R G, Thakur O P and Prakash C 2002b *J. Appl. Phys.* **91** 6626
- Sooahoo R F 1960 *Theory and application of ferrites* (New Jersey: Prentice Hall) p. 109
- Tsakaloudi V, Papazoglou E and Zaspalis V T 2004 *Mater. Sci. Eng.* **B106** 289
- Wang F F W, Gravel R L and Kestigian M 1968 *IEEE Trans. Mags.* **MAG-4** 55
- White G O and Patton C R 1978 *J. Magn. Magn. Mater.* **9** 299
- Yadogi P, Peelameedu R, Agarwal D and Roy R 2003 *Mater. Sci. Eng.* **B98** 269